

Treatment of dye solutions by DL nanofiltration membrane

Duygu Kavak

Department of Chemical Engineering, Faculty of Engineering and Architecture, Eskişehir Osmangazi University, 26480, Meselik, Eskişehir, Turkey, Tel. +90 222 2393750, ext. 3645, Fax +90 222 2393613, email: dbayar@ogu.edu.tr

Received 23 July 2016; 13 October 2016

ABSTRACT

This study describes the rejection of acid black 194 dye using a DL nanofiltration membrane. Membrane experiments were conducted in a cross-flow system. Effects of membrane pressure (5, 10, and 15 bar), feed pH (3, 7, and 10), feed temperature (25, 35, and 45°C) and dye concentration in the feed solution (50, 500, and 1000 mg/L) on the membrane performance were investigated. The surface morphologies of membranes were investigated using scanning electron microscopy (SEM). The results indicate that the DL membrane has satisfactory average dye rejection ($99.72 \pm 0.140\%$) at operating pressure of 5 bar, 1000 mg/L dye concentration, 25°C feed temperature and feed pH = 7.

Keywords: Acid black 194; Cross-flow system; DL membrane; Nanofiltration

1. Introduction

Dye using industries such as textile, leather, and dye manufacturing generally require huge quantities of water for dyeing process [1–4]. According to their structural characteristics, dyes can be classified as acidic, basic, disperse, azo, diazo, anthraquinone based and metal complex [5]. Acid black 194 (AB194) is categorized as a highly toxic metal complex dye. Use of acid black 194 dye is very common in blended fabric dyeing, direct printing in wool, silk fabric fiber and nylon non-woven micro fabric and leather dyeing [6,7]. Wastewaters contaminated with dyes, severely threaten human health and have both toxic and mutagenic effects on organisms because of the carcinogenic nature of dye. To prevent hazardous effects of wastewaters containing dye, they should be treated before being released into environment [8]. For the removal of dye from wastewater there are conventional methods such as adsorption [9–11], ion exchange [12,13], chemical oxidation [14,15], coagulation/flocculation [16], electrocoagulation/flotation [17] and biosorption [18,19]. There are advantages and disadvantages of these methods. Choice of method depends on objectives to be achieved [20]. Membrane techniques have

proven to be very attractive and effective for wastewater treatment. The main advantage of membrane processes is that there is no need for adding any chemicals. The most common membrane separation methods are microfiltration (MF), ultrafiltration (UF), nanofiltration (NF) and reverse osmosis (RO) [21,22]. In treatment of textile wastewater mostly nanofiltration is used for its unsurpassed separation features [23]. There is less fouling problem in NF compared to RO. Moreover, NF has a higher rejection efficiency than UF [24,25]. Due to these advantages, NF technology is used for drinking water production, recovery of heavy metals, eliminating dyes, small organics, dissolved organics molecules, pharmaceutical compounds, and pesticides from water [26,27].

Dye removal from water with the NF process has been investigated in the previous studies, but there is a lack of reports on removal of acid black 194 using NF process by DL membrane. The main goal of this work is to evaluate the separation of DL membrane under various operating conditions such as membrane pressure, feed pH, feed temperature and initial dye concentration. The dye rejection values and permeate flux were determined in different operation conditions.

Presented at the EDS conference on Desalination for the Environment: Clean Water and Energy, Rome, Italy, 22–26 May 2016.

2. Materials and methods

2.1. Materials

Acid black 194 was used in the experiments. The dye was supplied by Burboya Co Textile Industry, Bursa, Turkey. The chemical structure and characteristics of AB194 are shown in Table 1. The nanofiltration membrane used in this study was a DL membrane supplied by GE Osmonics, Florida, USA as a flat sheet, thin-film nanofiltration membrane. DL membranes had an active layer consisting of the poly-piperazine amide (PA) [28]. Table 2 gives the specifications of the membrane provided by the manufacturer [29].

2.2. Filtration experiments

Membrane experiments were conducted in a cross-flow test system (SEPA CF, Sterlitech) as shown in Fig. 1. This system is formed by a membrane module, a hydraulic hand pump, a feed tank, a high pressure pump, an analytical balance for the measurement of flux, a computer, a thermostat, a flowmeter, and other necessary fittings. The stainless steel cross-flow filtration system had a total volume of 5 L and contained an effective membrane area of 0.015 m². Synthetic wastewater taken from feed tank by centrifugal pump was transmitted to the membrane cell. Amount of permeate was measured by an analytical balance which was connected to the computer. The weight of the collected permeate was monitored at 1 min intervals. Each dye rejection test was performed in triplicate and the results presented were average data with standart deviation. Accordingly error bar was put in the figures as well. The temperature was maintained constant at 25°C by a thermostat during the filtration test. Aqueous solutions prepared by dissolving dye (1000 mg/L) in deionized water were used for the filtration study.

2.3. Data analyses

The permeate flux (J) is determined by using Eq. (1):

$$J = \frac{Q}{A \cdot t} \quad (1)$$

where Q , A and t are the volume of permeate (L), effective area of the membrane (m²), and filtration time (h), respectively [21].

The dye concentrations of the feed and permeate were analyzed by using a UV-vis spectrometer (Shimadzu, model UV-120-01) at the λ_{\max} value of 570 nm for AB194.

The rejection (R) value of dye is calculated as follows:

$$R = \left(1 - \frac{C_p}{C_f}\right) \times 100\% \quad (2)$$

where C_p (mg/L) and C_f (mg/L) represent the dye concentrations in the permeate and in the feed solution, respectively.

2.4. Scanning electron microscopy

The surface morphologies of DL membrane samples were imaged using a JEOL-JSM-5600 LV scanning electron microscope (SEM). The samples were gold-palladium coated prior to SEM observation. The SEM images were collected with a beam potential of 20 kV

3. Results and discussion

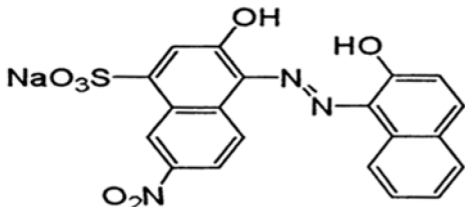
3.1. Effects of operating pressure

The fluxes of DL membrane as a function of pressure are shown in Fig. 2. As presented in this figure, pressures of 5 to 15 bars were applied. The permeate flux increased with increasing pressure. For example, the permeate flux increases from 45 to 57 L/m² h (27% flux enhancement) as membrane pressure increases from 5 to 15 bar. This is a result of the driving forces increasing with the increased operating pressure and overcoming the resistance of the membrane [30]. The steady-state permeate flux values for dye rejection using DL with 5, 10, and 15 bars were 45, 54, and 57 L/m² h, respectively. It can be seen from the figure that the water fluxes decrease with filtration time at 10 and 15 bars. The decline of flux is mainly due to the deposition and adsorption of foulants on the membrane surface [1,31]. For example, at 10 bar pressure, the permeate flux declines from 59 L/m² h to 54 L/m² h (decrease of 8.5%). At 15 bar

Table 2
Commercial DL membrane specifications [29]

Membrane	Description
Manufacturer	GE Osmanics (USA)
Molecular Weight Cut-off (Da)	~150–300
pH tolerance	2–10
Polimer	Thin-film
MgSO ₄ Rejection (%)	98.00
Type	Low energy, low pressure

Table 1
Characteristics of AB194 [6]

Chemical structure	Molecular formula	λ_{\max} (nm)	Molecular weight (g/mol)
	C ₂₀ H ₁₂ N ₃ NaO ₇ S	570	461.38

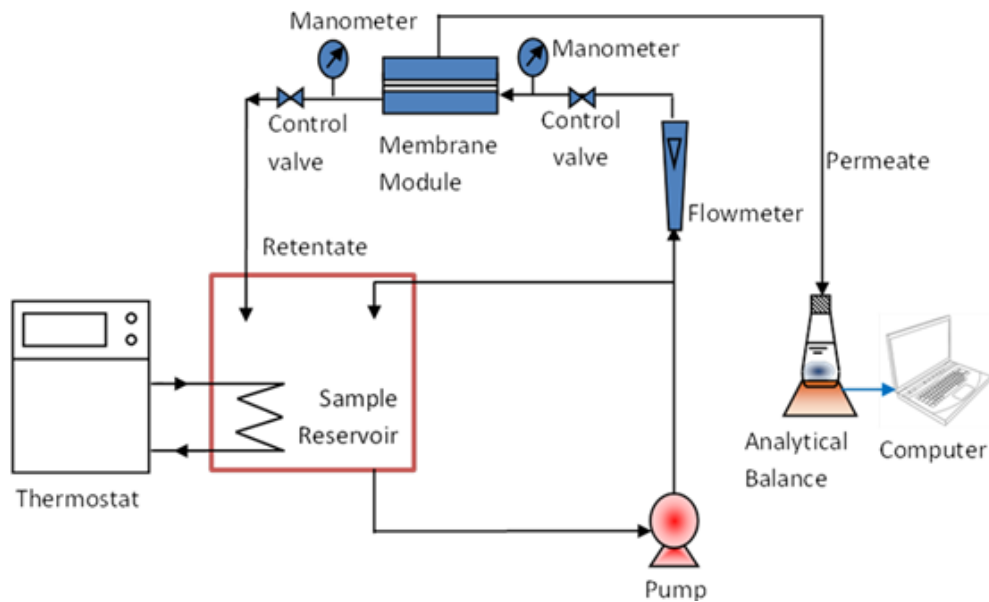


Fig. 1. Schematic drawing of the experimental cross-flow filtration unit.

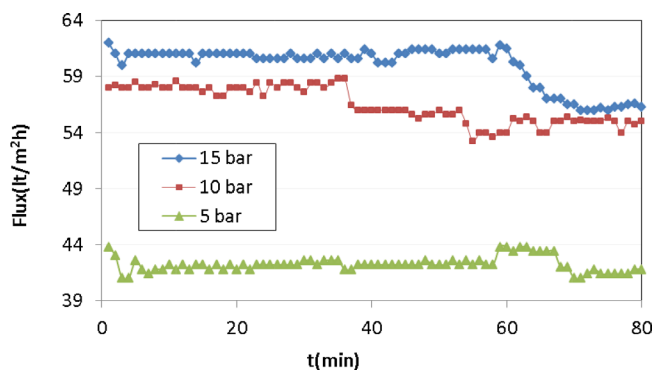


Fig. 2. Effect of pressure on permeate fluxes of DK membrane (feed temperature: 25°C, initial dye concentration = 50 ppm, pH = 7).

pressure the permeate flux decline is 62 L/m² h to 57 L/m² h (decrease of 8.1%). No flux decline is observed at 5 bar. Koyuncu [3] also reported increase in permeate flux with increasing pressure using the DS5 DK type nanofiltration membrane for removal of Reactive Black5, Reactive Orange16, Reactive Blue19.

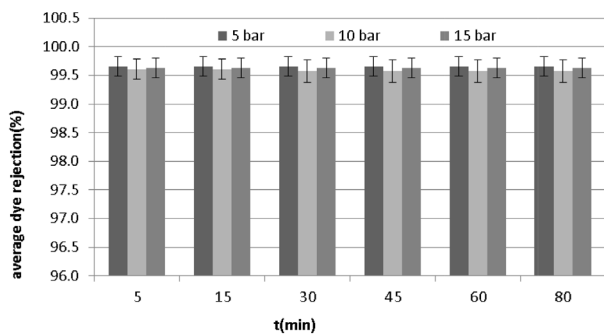


Fig. 3. Effect of pressure on the rejection of AB194 dye (feed temperature: 25°C, initial dye concentration = 50 ppm, pH = 7).

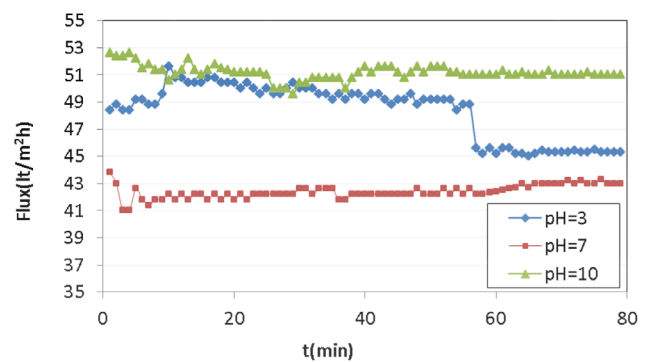


Fig. 4. Effect of feed pH on permeate fluxes of DK membrane (pressure: 5 bar, feed temperature: 25°C, initial dye concentration = 50 ppm).

Fig. 3 shows the variation of the metal rejection (%) as a function of transmembrane pressure (ΔP). As shown in Fig. 3, the average dye rejection percentages of DL membrane are above $99.57 \pm 0.197\%$ for all pressure values tested in the experiments.

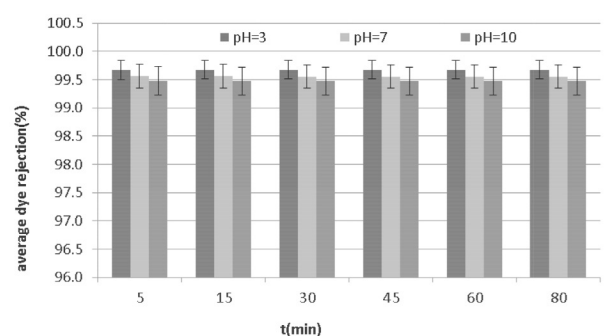


Fig. 5. Effect of feed pH on the rejection of AB194 dye (pressure: 5 bar, feed temperature: 25°C, initial dye concentration = 50 ppm).

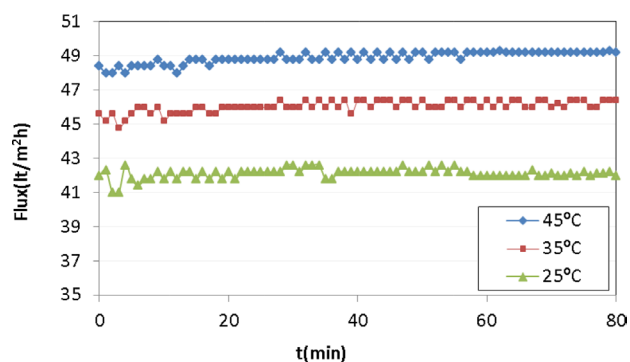


Fig. 6. Effect of feed temperature on permeate fluxes of DK membrane (pressure: 5 bar, initial dye concentration = 50 ppm, pH = 7).

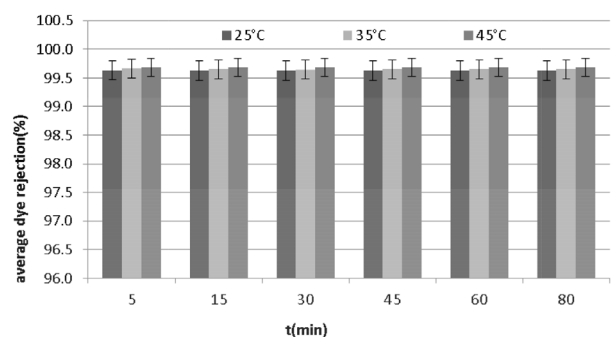


Fig. 7. Effect of feed temperature on the rejection of AB194 dye (pressure: 5 bar, initial dye concentration = 50 ppm, pH = 7).

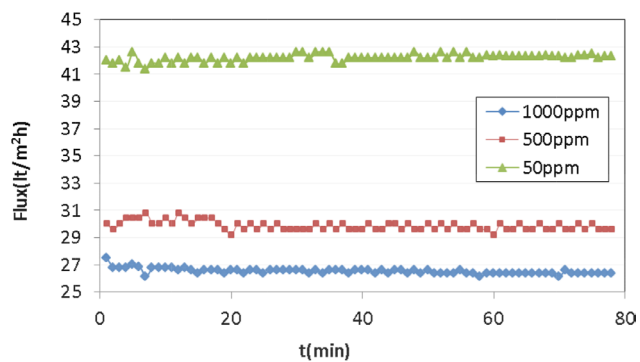


Fig. 8. Effect of initial feed concentration on permeate fluxes of DK membrane (pressure: 5 bar, feed temperature: 25°C, pH = 7).

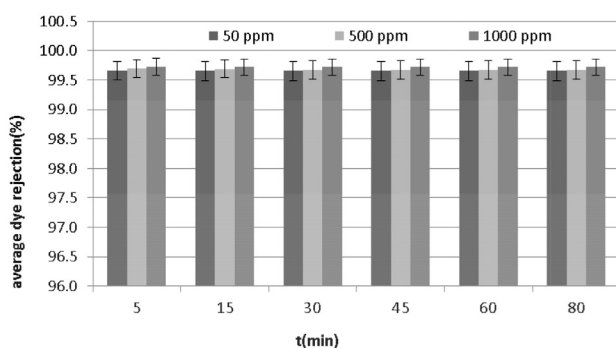


Fig. 9. Effect of initial feed concentration on the rejection of AB194 dye (pressure: 5 bar, feed temperature: 25°C, pH = 7).

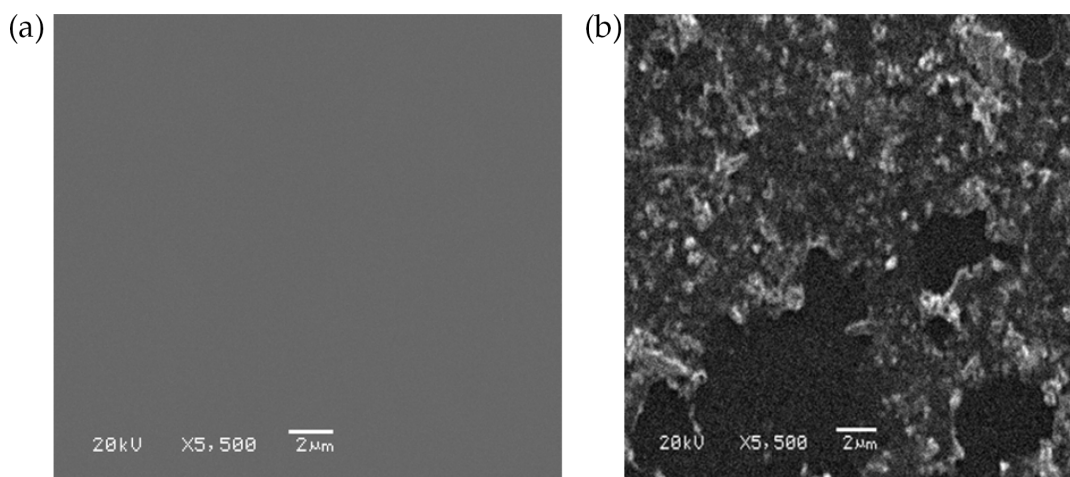


Fig. 10. SEM images of DL membranes (a) Fresh DL membrane and (b) The fouled DL membrane after the nanofiltration process (pressure: 5 bar, initial dye concentration = 50 ppm, pH = 7).

3.2. Effects of feed pH

The effect of feed pH on the permeate flux and the rejection parameters in synthetic wastewater containing AB194 were determined by DL membrane at 3, 7 and 10 pH levels at 5 bar pressure, 50 mg/L dye concentration, 25°C temperature. As seen from the Fig. 4, at pH = 3 decrease was observed in permeate flux after 55 min. There were no significant declines at pH = 7 and pH = 10. The charge on

membrane surface may be affected by the changes of feed pH values. According to the Religa et al. [32] the isoelectric point (IP) was 3.0 for DL membrane. The higher rejection at IP (pH = 3) as at this point the electrostatic interaction between the membrane and the dye was zero. Therefore, the dye did not easily permeate the membrane [33]. The isoelectric point of used NF membrane is at 3.0 above which the membrane becomes negatively charged, resulting in

Table 3
Dye rejection comparison NF membranes in the literature and this study

Dye	Membrane	Operating condition	Dye rejection (%)	Ref.
Reactive Black 5	Polysulfone-polyamide, DS5 DK	8–24 bar, 0.74 m/s	>99.00 ^a	[3]
Reactive Orange16	Polysulfone-polyamide DS5 DK	8–24 bar, 1000 mg/L dye, 0.74 m/s	>99.00 ^a	[3]
Reactive Blue 19	Polysulfone-polyamide, DS5 DK	8–24 bar, 1000 mg/L dye, 0.74 m/s	>99.00 ^a	[3]
Direct Red 75,80,81, Direct Yellow 8,27	Polyamide (PA) composite membrane	1000 mg/L dye	>99.50 ^a	[4]
Reactive red 198	Polypiperazine amide, (PA-NF) Polyether sulfone,(PES)	4.9 bar, 25 mg/L dye, 500 mg/L salt	99.55 ^a 99.83 ^a	[24]
Congo red	Polypiperazine amide, (PA-NF)	20 mg/L dye, pH 9	100.00 ^a	[26]
Direct Red 80	Sepro NF 2A	6 bar,100 mg/L	99.98 ± 0.02 ^a	[27]
Direct Red 23	Sepro NF 2A	6 bar, 100 mg/L	99.95 ± 0.02 ^a	[27]
Congo Red	Sepro NF 2A	6 bar, 100 mg/L	99.96 ± 0.03 ^a	[27]
Direct Red 80	Sepro NF 6	6 bar, 100 mg/L	99.95 ± 0.02 ^a	[27]
Direct Red 23	Sepro NF 6	6 bar, 100 mg/L	99.76 ± 0.03 ^a	[27]
Congo Red	Sepro NF 6	6 bar, 100 mg/L	99.93 ± 0.03 ^a	[27]
Reactive Yellow 81 Reactive Black 5 Reactive Blue 19	Polyamide-imide NF	All testing conditions	>98.00 ^a	[34]
Acid Red 114	Spiral wond, NF	200 mg/L dye, 1000 mg/L NaCl	98.16 ^a	[37]
Everzol Black + NaCl	Polyamide, NF-200	15 bar, 600 mg/L dye, 500 mg/L NaCl	98.43 ^a	[38]
Everzol Black + NaCl	Polyamide, NF-270	15 bar, 600 mg/L dye, 500 mg/L NaCl	99.22 ^a	[38]
Everzol Red + NaCl	Polyamide, NF-200	15 bar, 600 mg/L dye, 500 mg/L NaCl	97.07 ^a	[38]
Everzol Red + NaCl	Polyamide, NF-270	15 bar, 600 mg/L dye, 500 mg/L NaCl	97.91 ^a	[38]
Everzol Blue + NaCl	Polyamide NF-200	15 bar, 600 mg/L dye, 500 mg/L NaCl	98.51 ^a	[38]
Everzol Blue + NaCl	Polyamide, NF-270	15 bar, 600 mg/L dye, 500 mg/L NaCl	100.00 ^a	[38]
Cibacron Yellow	Polysulfone, PSF	5.5 bar, 120 L/h	98.50 ^a	[39]
Cibacron Red	Polysulfone, PSF	5.5 bar, 120 L/h	99.90 ^a	[39]
Cibacron Black	Polysulfone, PSF	5.5 bar, 120 L/h	99.80 ^a	[39]
Cibacron Blue	Polysulfone, PSF	5.5 bar, 120 L/h	99.70 ^a	[39]
Reactive Black 5	Hollow fiber NF	0.8 bar, 32 mg/L dye	>99.80 ^a	[40]
Orange II, Remazol	NF-1 (protective layer)	1bar, 50 mg/L dye	>99.00 ^a	[41]
Brilliant Blue R	NF-1 (without protective layer)			
Safranin O	NF 1	50 mg/L dye	99.60 ± 0.02 ^a	[42]
	NF 2		99.68 ± 0.02 ^a	
Orange II	NF 1	50 mg/L dye	59.67 ± 3.29 ^a	[42]
	NF 2		99.68 ± 2.52 ^a	
Acid Black 194	Thin-film, DL	5 bar, 1000 mg/L dye, pH 7, 25°C	99.72 ± 0.14	This work

^adata redrawn from references.

an enhancement in the electrical repulsive force (Donnan exclusion) between the membrane and dye. Minimum fouling was observed at pH = 10.

Fig. 5 shows the variation of the dye rejection (%) as a function of feed pH. As shown in this figure, the rejection of the dye slightly increased with decreasing pH. Average dye rejection percentages were obtained as 99.67 ± 0.166%, 99.55 ± 0.209% and 99.47 ± 0.247% for 3, 7 and 10 pH values, respectively.

3.3. Effects of feed temperature

The performance of the DL membrane was investigated at various feed temperatures (25, 35, 45°C). The obtained

results were presented in Fig. 6. According to Fig. 6, the flux increases with an increase in feed temperature. As the feed temperature was increased from 25 to 45°C, the permeate flux increased from 42 L/m² h to 49 L/m² h, respectively. This behavior is attributed to the decrease in the viscosity which leads to the increase of the mass transfer coefficient [34]. A similar increase in permeate flux with increasing temperature was also reported by Ong et al. [34] and Ellouze et al. [35].

As shown in Fig. 7 with the increase of temperature, the dye rejection of DL membrane increased slightly. Average dye rejection percentages were found as 99.62 ± 0.169%, 99.65 ± 0.162% and 99.69 ± 0.158% at 25, 35 and 45°C, respectively.

3.4. Effects of initial dye concentration

The membrane performance as a function of dye concentration was investigated. Experiments were conducted at 50, 500, and 1000 mg/L dye concentrations. The results are shown in Figs. 8 and 9. As can be seen in Fig. 8, the permeate flux decreases with increasing dye concentration because increasing dye concentration results in increase of polarization and dye adsorption on the membrane surface. The results confirm with that of Ji et al. [36] and Al-Aseeri et al. [37]. The effect of dye concentration on dye removal is shown in Fig. 9. Very high percentage of average dye rejections (over $99.65 \pm 0.160\%$) were observed at all concentrations of dyes. As can be seen from Fig. 9, when the concentration of dye increased the rejection of dye also increased but not significantly. Ji et al. [36] also reported that increasing dye concentration would not affect dye rejection significantly and explained this with good mass transfer across the membrane surface which prevents serious concentration polarization.

3.5. SEM micrograph analysis

SEM image of top surface of fresh membrane was shown in Fig. 10(a) at 5500x magnification. After the nanofiltration process, the fouled DL membrane was observed by SEM, which was presented in Fig. 10(b) at the same magnification. According to Fig. 10(b), there are deposits of some dye molecules on the membrane surface, which also led to the decrease of permeate flux.

3.6. The comparison among rejection of AB194 and rejection of other dyes by different NF membranes

Comparison of average acid black 194 rejection ($99.72 \pm 0.140\%$) observed in this study with other dye rejection values of various NF membranes in the literature is given in Table 3. It can be concluded from Table 3 that NF membranes have a high dye rejection ($>97.00\%$).

4. Conclusions

The performance of DL nanofiltration membrane to remove acid black dye from model solutions is studied in this paper. The influence of operational variables such as membrane pressure, feed pH, feed dye concentration and feed temperature on rejection and permeate flux has been investigated. The permeate flux increases as the pressure and the feed temperature go up. However, the higher the dye concentration, the lower the flux is. The membrane shows a higher flux in an alkaline feed solution (pH = 10). The average dye rejection is independent of the operating conditions and remains high ($>99.47 \pm 0.247\%$) at all testing conditions. This study demonstrated that AB194 dye can be successfully treated using DL membrane.

Acknowledgements

In this study, devices and tools bought by Eskişehir Osmangazi University Research Foundation were used (Project Number: 201215031). Acid black dye were supplied by Burboya.

References

- [1] P. Banerjee, S. De, Steady state modeling of concentration polarization including adsorption during nanofiltration of dye solution, *Sep. Purif. Technol.*, 71 (2010) 128–135.
- [2] S. Chakraborty, M.K. Purkait, S. DasGupta, S. De, J.K. Basu, Nanofiltration of textile plant effluent for color removal and reduction in COD, *Sep. Purif. Technol.*, 31 (2003) 141–151.
- [3] İ. Koyuncu, Reactive dye removal in dye/salt mixtures by nanofiltration membranes containing vinylsulphone dyes: Effects of feed concentration and cross flow velocity, *Desalination*, 143 (2002) 243–253.
- [4] J.H. Mo, Y.H. Lee, J. Kim, J.Y. Jeong, J. Jegal, Treatment of dye aqueous solutions using nanofiltration polyamide composite membranes for the dye wastewater reuse, *Dyes Pigm.*, 76 (2008) 429–434.
- [5] E.H. Ezechi, S.R.B.M. Kutty, A. Malakahmad, M.H. Isa, Characterization and optimization of effluent dye removal using a new low cost adsorbent: Equilibrium, kinetics and thermodynamic study, *Process Saf. Environ.*, 98 (2015) 16–32.
- [6] <http://www.worlddyevariety.com/acid-dyes/acid-black-194.html>
- [7] R. Sebastiano, N. Contiello, S. Senatore, P.G. Righetti, A. Citterio, Analysis of commercial Acid Black 194 and related dyes by micellar electrokinetic chromatography, *Dyes Pigm.*, 94 (2012) 258–265.
- [8] S.K. Maurya, K. Parashuram, P.S. Singh, P. Ray, A.V.R. Reddy, Preparation of polysulfone–polyamide thin film composite hollow fiber nanofiltration membranes and their performance in the treatment of aqueous dye solutions, *Desalination*, 304 (2012) 11–19.
- [9] C. Srilakshmi, R. Saraf, Ag-doped hydroxyapatite as efficient adsorbent for removal of Congo red dye from aqueous solution: Synthesis, kinetic and equilibrium adsorption isotherm analysis, *Micropor. Mesopor. Mat.*, 219 (2016) 134–144.
- [10] S. Karimifard, M.R.A. Moghaddam, Enhancing the adsorption performance of carbon nanotubes with a multistep functionalization method: Optimization of Reactive Blue 19 removal through response surface methodology, *Process Saf. Environ.*, 99 (2016) 20–29.
- [11] A. Reffas, A. Bouguettoucha, D. Chebli, A. Amrane, Adsorption of ethyl violet dye in aqueous solution by forest wastes, wild carob, *Desal. Water Treat.*, 57 (2016) 9859–9870.
- [12] J. Fan, H. Li, C. Shuang, W. Li, A. Li, Dissolved organic matter removal using magnetic anion exchange resin treatment on biological effluent of textile dyeing wastewater, *J. Environ. Sci.*, 26 (2014) 1567–1574.
- [13] M. Wawrzkiwicz, Z. Hubicki, Kinetics of adsorption of sulphonated azo dyes on strong basic anion exchangers, *Environ. Technol.*, 30(10) (2009) 1059–1071.
- [14] M.A. Wasim, R. Ullah, N.M. AbdEl-Salam, S. Ayaz, Gamma radiation induced decolorization of an aqueous textile dye solution in the presence of different additives, *Desal. Water Treat.*, 55 (2015) 1945–1955.
- [15] O. Gokkus, F. Coskun, M. Kocaoglu, Y.S. Yildiz, Determination of optimum conditions for color and COD removal of Reactive Blue 19 by Fenton oxidation process, *Desal. Water Treat.*, 52 (2014) 6156–6165.
- [16] K.L. Yeap, T.T. Teng, B.T. Poh, N. Morad, K.E. Lee, Preparation and characterization of coagulation/flocculation behavior of a novel inorganic–organic hybrid polymer for reactive and disperse dyes removal, *Chem. Eng. J.*, 243 (2014) 305–314.
- [17] G.R. Mohammed, T.M. Zewail, Y.A. El-Tawail, Optimization of color removal from two types of anionic dyes by electrocoagulation/flotation in a batch agitated vessel, *Desal. Water Treat.*, 52 (2014) 6684–6693.
- [18] S.Y. Kim, M.R. Jin, C.H. Chung, Y.-S. Yun, K.Y. Jahng, K.-Y. Yu, Biosorption of cationic basic dye and cadmium by the novel biosorbent *Bacillus catenulatus* JB-022 strain, *J. Biosci. Bioeng.*, 119(4) (2015) 433–439.
- [19] E. Tomczak, W. Kaminski, P. Tosik, Adsorption dynamics studies of azo dyes removal by biosorbent, *Desal. Water Treat.*, 55 (2015) 2669–2674.

- [20] S. Karmakar, M. Mondal, S. Ghosh, S. Bandyopadhyay, S. Majumdar, S. De, Removal of reactive dyes using a high throughput-hybrid separation process, *Desal. Water Treat.*, 157 (2016) 10295–10311.
- [21] M. Amini, M. Arami, N.M. Mahmoodi, A. Akbari, Dye removal from colored textile wastewater using acrylic grafted nanomembrane, *Desalination*, 267 (2011) 107–113.
- [22] A. Ammar, I. Dofan, V. Jegatheesan, S. Muthukumar, L. Shu, Comparison between nanofiltration and forward osmosis in the treatment of dye solutions, *Desal. Water Treat.*, 54 (2015) 853–861.
- [23] Y. Zheng, S. Yu, S. Shuai, Q. Zhou, Q. Cheng, M. Liu, C. Gao, Color removal and COD reduction of biologically treated textile effluent through submerged filtration using hollow fiber nanofiltration membrane, *Desalination*, 314 (2013) 89–95.
- [24] T.M. Patel, K. Nath, Performance of polyamide and polyethersulfone membranes in the nanofiltration of reactive dye-salt mixtures on pilot scale, *Desal. Water Treat.*, 52 (2014), 7026–7036.
- [25] N. Askari, M. Farhadian, A. Razmjou, H. Hashtroodi, Nanofiltration performance in the removal of dye from binary mixtures containing anthraquinone dyes, *Desal. Water Treat.*, 57 (2016) 18194–18201.
- [26] N.H.H. Hairom, A.W. Mohammad, A.A.H. Kadhum, Nanofiltration of hazardous Congo red dye: Performance and flux decline analysis, *J. Wat. Proc. Engin.*, 4 (2014) 99–106.
- [27] J. Lin, W. Ye, H. Zeng, H. Yang, J. Shen, S. Darvishmanes, P. Luis, A. Sotro, B.V.D Bruggen, Fractionation of direct dyes and salts in aqueous solution using loose nanofiltration membranes, *J. Membr. Sci.*, 477 (2015) 183–193.
- [28] P. Religa, A. Kowalik-Klimczak, P. Gierycz, Study on the behavior of nanofiltration membranes using for chromium(III) recovery from salt mixture solution, *Desalination*, 315 (2013) 115–123.
- [29] <http://www.sterlitech.com/membrane-process-development/flat-sheet-membranes>
- [30] G. Basaran, D. Kavak, N. Dizge, Y. Asci, M. Solener, B. Ozbey, Comparative study of the removal of nickel(II) and chromium(VI) heavy metals from metal plating wastewater by two nanofiltration membranes, *Desal. Water Treat.*, 57(46) (2016) 21870–21880.
- [31] X. Wei, X. Kong, S. Wang, H. Xiang, J. Wang, J. Chen, Removal of heavy metals from electroplating wastewater by thin-film composite nanofiltration hollow-fiber membranes, *Ind. Eng. Chem. Res.*, 52 (2013) 17583–17590.
- [32] P. Religa, A. Kowalik, P. Gierycz, Effect of membrane properties on chromium(III) recirculation from concentrate salt mixture solution by nanofiltration, *Desalination*, 274 (2011) 164–170.
- [33] B.A.M. Al-Rashdi, D.J. Johnson, N. Hilal, Removal of heavy metal ions by nanofiltration, *Desalination*, 315 (2013) 2–17.
- [34] Y.K. Ong, F.Y. Li, S.-P. Sun, B.-W. Zhao, C.-Z. Liang, T.-S. Chung, Nanofiltration hollow fiber membranes for textile wastewater treatment: Lab-scale and pilot-scale studies, *Chem. Eng. Sci.*, 114 (2014) 51–57.
- [35] E. Ellouze, N. Tahri, R.B. Amar, Enhancement of textile wastewater treatment process using nanofiltration, *Desalination*, 286 (2012) 16–23.
- [36] L. Ji, Y. Zhang, E. Liu, Y. Zhang, C. Xiao, Separation behavior of NF membrane for dye/salt mixtures, *Desal. Water Treat.*, 51 (2013) 3721–3727.
- [37] M. Al-Aseeri, Q. Bu-Ali, S. Haji, N. Al-Bastaki, Removal of Acid Red and sodium chloride mixtures from aqueous solutions using nanofiltration, *Desalination*, 206 (2007) 407–413.
- [38] A. Aouni, C. Fersi, B. Cuartas-Urbe, A. Bes-Piá, M.I. Alcaina-Miranda, M. Dhahbi, Study of membrane fouling using synthetic model solutions in UF and NF processes, *Chem. Eng. J.*, 175 (2011) 192–200.
- [39] S.R. Panda, S. De, Performance evaluation of two stage nanofiltration for treatment of textile effluent containing reactive dyes, *J. Environ. Chem. Eng.*, 3 (2015) 1678–1690.
- [40] X. Zhu, Y. Zheng, Z. Chen, Q. Chen, B. Gao, S. Yu, Removal of reactive dye from textile effluent thorough submerged filtration using hollow fiber composite nanofiltration membrane, *Desal. Water Treat.*, 51 (2013) 6101–6109.
- [41] Y.K. Ong, T-S. Chung, Mitigating the hydraulic compression of nanofiltration hollow fiber membranes through a single-step direct spinning technique, *Environ. Sci. Technol.*, 48 (2014) 13933–13940.
- [42] P.S. Zhong, N. Widjojo, T-S. Chung, M. Weber, C. Maletzko, Positively charged nanofiltration (NF) membranes via UV grafting on sulfonated polyphenylenesulfone (sPPSU) for effective removal of textile dyes from wastewater, *J. Membr. Sci.*, 417–418 (2012) 52–60.